Article citation info:
Kozhushko A, Kravchenko S, Shuliak M, Kolesnik I, Danylenko V. Analysis of fuel economy indicators of a wheeled tractor during transportation of partially filled tankers. Combustion Engines. 0000;XXX(X):xx-xx. https://doi.org/10.19206/CE-220540

Andrii KOZHUSHKO
Serhii KRAVCHENKO
Mykhailo SHULIAK
Ivan KOLESNIK
Vitalii DANYLENKO

Combustion Engines
Polish Scientific Society of Combustion Engines

Analysis of fuel economy indicators of a wheeled tractor during transportation of partially filled tankers

ARTICLE INFO

Received: 9 January 2026
Revised: 11 March 2026
Accepted: 10 April 2026
Available online: 22 April 2026

This study examines the fuel performance characteristics of a wheeled tractor transporting a trailer tank under varying load conditions within standardized driving cycles (ELR, EPA, and NRTC). A mathematical model of the tractor–trailer system was developed in MATLAB/Simulink, incorporating the dynamics of the FPT NEF 67 internal combustion engine, the transmission and wheel drives, as well as the effects of fluid redistribution in the tank. The model enables evaluation of instantaneous fuel consumption, specific fuel consumption, effective power, and engine efficiency under dynamic operating modes. Particular attention is given to the impact of fluid sloshing on energy expenditure, which is most pronounced at a tank fill height of 1.3 m (out of 1.6 m), corresponding to resonance conditions. The results demonstrate that the dynamic characteristics of the driving cycles have a significant impact on additional fuel consumption: NRTC yields the highest relative increase (9.22%), EPA the highest absolute increase (6.76%), and ELR the lowest (4.72%). These findings provide a basis for optimizing tractor operation during liquid cargo transport and for assessing the potential benefits of hybridizing tractor transmission systems in transport applications.

Key words: *tractor, engine, transport work, tank, free surface of liquid, fuel consumption, fuel efficiency, driving cycles, simulation*

1. Introduction

Transport operations constitute an important component of the operational load of wheeled tractors in the agro-industrial complex. Within the overall cycle of agricultural activities, a tractor performs not only traction-based soil cultivation and operation with tillage implements, but also a significant volume of intra-farm and inter-farm transportation tasks. These include the collection and transportation of grain, root crops, and green fodder; the delivery of fertilizers, spare parts, and tools; and the organization of logistical operations during the harvesting period. According to field studies and technical surveys conducted across various countries, the share of transport operations in tractors' annual operating time can be substantial and varies by region, farm type, and machinery structure. In a number of analyses, transport operations account for approximately 10–60% of annual engine operating hours for certain tractor categories (low-power and general-purpose), especially in regions with fragmented fields and intensive intra-farm logistics. The use of agricultural tractors for road transport may result in significantly higher fuel consumption than conventional transport vehicles, indicating the need to analyze their fuel efficiency in transport operations [13].

According to data reported in [1], agricultural regions of Europe characterized by small and medium-sized farms allocate about 30–60% of annual tractor operating hours to transport operations. This is explained by the fact that many European studies of tractor duty cycles indicate a high proportion of travel, idling, and short-distance transport between fields in daily operation, particularly in areas with fragmented land use [6]. In regions with smallholder farming systems in China, the share of transport operations is approximately 20–50%; in particular, in southern and eastern provinces, this share is higher due to frequent transportation between small fields and local storage facilities, whereas in large agro-industrial complexes of northern and northeastern China, the proportion of transport cycles is generally lower. A review of mechanization and tractor electrification trends in China [20] confirms significant variability in tractor usage profiles. In the United States, transport operations account for approximately 10–30% of total tractor operating hours [17]. This situation is explained by the fact that many transport functions – such as long-distance logistics and transportation between fields – are performed by specialized trucks and truck combinations, while tractors are more frequently used for field operations with prolonged continuous loads (tillage, planting, harvesting). As a result, the share of purely transport-related operating hours is typically lower than in small European farms.

Transport operations performed by wheeled tractors include all activities [11] related to the movement of cargo, raw materials, supplies, machinery, or auxiliary equipment within a farm or beyond its boundaries. These operations involve delivering seeds to seeders, transporting mineral and organic fertilizers, plant protection products, and water for spraying, and supplying feed in livestock complexes. In addition, tractors are used to transport harvested crops – grain, root crops, and green biomass – from the harvester to the field edge or temporary storage, and subsequently to elevators, warehouses, or processing facilities. Transport operations also include technological transport within tractor–trailer combinations [1, 8, 12, 18], such as towing fertilizer spreader trailers, feed distribution wagons, or grain transfer carts during harvesting. Furthermore, tractors perform auxiliary logistical functions, including the transportation of fuel, technical fluids, spare parts, and tools, the delivery of maintenance crews, or the recovery of disabled machinery. With the increasing volume of intra-farm trans-

portation, the intensification of agricultural production, the expansion of cultivated areas, and the spatial dispersion of land plots, the role of transport operations in the overall technical load structure of tractors continues to grow.

2. Literature review

One of the most common types of transport operations performed by wheeled tractors in agriculture is the transportation of liquid loads in trailed or semi-trailed tanks [2, 10], including liquid organic fertilizers, manure effluents, irrigation water, working solutions of pesticides, and other agrochemicals. Unlike the transportation of bulk or unit (solid) cargo, the transportation of liquid loads is characterized by the presence of internal dynamic disturbances caused by the motion of the liquid inside a cylindrical tank [15]. Such oscillations lead to variations in loads transmitted through the drawbar coupling to the tractor axle and the power unit.

The disturbing forces generated by oscillations of the liquid mass significantly affect the dynamics of the tractor unit: they increase the amplitude of vertical and angular vibrations, alter the distribution of normal reactions on the supporting wheels, and reduce stability during braking and maneuvering. In the case of uneven field roads, slopes, or increased transport speed, the liquid load may generate resonant wave processes, increasing the risk of tank rollover or loss of tractor controllability. This is particularly critical for large-capacity machines (10–18 m³ and more) and for tractor-tank combinations with a total mass exceeding 15 t [12].

An additional challenge of modern agricultural production is the tendency toward increasing volumes of liquid fertilizer transportation within the framework of precision farming technologies and environmentally sound fertilization practices. This leads to higher transport speeds and increased tractor loads. At the same time, from a safety standpoint, tractor-tank aggregates (the "tractor-tank" system) remain significantly less studied than road vehicles, despite substantial accident rates and equipment downtime. Study [19] demonstrates that at high speeds and high tank filling levels, the mass center position shifts, leading to a noticeable increase in lateral and torsional moments. It was established that tank filling levels between 70–90% have the most adverse effect on braking performance and dynamic stability. Furthermore, [9] shows that the greatest liquid sloshing forces occur in tractor tanks filled at 71–92%, a hazardous level that affects not only productivity but also traffic safety.

The evaluation of the fuel characteristics of an internal combustion engine based on its load characteristics is driven by its dynamic operation and the diversity of operating conditions. Fuel economy depends not only on the engine design but also on its response to changes in load and operating modes. Load characteristics reflect real operating conditions and enable the assessment of variations in specific fuel consumption and effective efficiency, as well as the determination of the engines best fuel-economy range [7].

During numerical simulation of wheeled tractor motion, an important aspect is selecting an appropriate driving test cycle that reproduces the characteristic operating modes of agricultural machinery. Modern practice [14, 16] employs several approaches to forming such cycles. In particular, the international regulatory framework (European Load Response [5], EPA Non-road Duty Cycles [3]) defines test cycles for various types of mobile agricultural and construction equipment, including wheeled tractors. These cycles are based on experimental data describing variations in the angular speed and effective torque of the internal combustion engine crankshaft, which closely reflect real operating conditions.

According to [1, 4], the NRTC cycle is appropriate for off-road specialized machinery, including agricultural tractors and construction equipment. It allows the simulation of load characteristics across a wide range of operating conditions, typical of both field work and operations involving frequent stops, accelerations, and periodic torque changes. Unlike steady-state characteristics, the NRTC includes a full sequence of realistic dynamic effects that occur during machine acceleration, idling, transitions to partial loads, or operation at short-term peak power levels. This structure enables accurate reproduction of transient modes, which dominate during the real operation of internal combustion engines under variable load conditions, when the powertrain continuously adapts to varying road conditions, changing soil conditions, or cyclical operation of mounted and towed implements.

The aim of this study is to provide a theoretical basis for determining changes in the fuel economy of a wheeled tractor during the transportation of liquid cargo with a free liquid surface by simulating standardized driving cycles.

3. Description of the ICE crankshaft motion

When describing changes in the operational performance of an internal combustion engine, a fairly common practice is to neglect the working processes by which the chemical energy of the fuel is converted into mechanical work. In addition, when describing the mechanical operation of the internal combustion engine, an assumption is introduced that the harmonic components of the torque are neglected. During engine operation, the torque on the crankshaft is a non-constant quantity that varies within each working cycle due to the alternation of strokes, changes in cylinder pressure, inertial forces of the valve train, and other factors. These fluctuations are periodic in nature and can be represented as the sum of an average (steady) torque and harmonic (pulsating) components.

Thus, the stated assumptions make it possible to use the equation of dynamic equilibrium of crankshaft motion:

$$J_e \cdot \frac{d\omega_e}{dt} = M_e + M_D \tag{1}$$

where: J_e – moment of inertia of the masses reduced to the crankshaft; ω_e – angular speed of the crankshaft; M_e – actual (effective) torque on the crankshaft; M_D – resistive torque accounting for the load from the transmission, auxiliary units, and friction losses.

Analyzing the equation reveals that it describes the dynamic equilibrium of a rotational system and generalizes Newton's second law to rotational motion. Its physical meaning lies in reflecting the relationship between the acting torques and the changes in the internal combustion engine's kinetic state. The left-hand side of the equation –

the product of the moment of inertia J_e and the angular acceleration $d\omega_e/dt$ – characterizes the torque required to change the angular speed of the crankshaft. In this case, the moment of inertia is a measure of the rotational system's inertial properties that resist changes in rotational speed. It includes not only the crankshaft itself, but also the flywheel, clutch components, and other parts kinematically connected to the engine.

The actual (effective) torque reflects the internal combustion engine's ability to generate rotational energy from fuel combustion in the cylinders. Its magnitude depends on the fuel supply mode, rotational speed, and other factors. The resistive torque determines the total opposition to rotation and includes mechanical losses, loads from the transmission and auxiliary units, and resistance arising from wheel interaction with the soil or road surface. Thus, the right-hand side of the equation represents the balance of torques acting on the crankshaft.

As shown, a major difficulty in modeling crankshaft motion is the representation of the actual torque component. To address this, it is proposed to introduce the parameter ε_r, which describes changes in the current position of the fuel supply control element. This approach simplifies the mathematical description, as neglecting the automatic control system significantly reduces the number of equations. Also note that the coefficient ε_r allows us to account for partial load in the internal combustion engine frequency and torque, since these can vary, $\varepsilon_r \in [0.46; 1]$.

$$\varepsilon_r = \frac{\omega_e}{\omega_{nom}} - \left(M_{normz} - \frac{M_e}{M_{nom}}\right) \cdot (k_x - 1) \qquad (2)$$

where: ω_{nom} – nominal angular speed of the crankshaft; M_{normz} – normalized torque; M_{nom} – nominal torque on the crankshaft; k_x – the coefficient defining the slope of the governor branch of the external speed characteristic.

Such terms of the equation as ω_{nom} and M_{nom} are tabulated values provided by the internal combustion engine manufacturer. The coefficient k_x is taken to be within the range of 1.07–1.086. The unknown term is the normalized torque, which depends on the external speed characteristic of the internal combustion engine, reduced to the nominal torque M_{nom}. Thus, under nominal operating conditions, when $M_e = M_{nom}$, the normalized torque equals $M_{normz} = 1$.

Next, a number of requirements are introduced that must be satisfied:

– the parameter ε_r is always smaller than the engine load coefficient with respect to rotational speed; they are equal only when:

$$M_{normz} = \frac{M_e}{M_{nom}} \qquad (3)$$

– the parameter $\varepsilon_r = \omega_e/\omega_{nom}$, when the maximum torque loading M_e/M_{nom} is equal to the normalized torque M_{normz};

– in cases where $\varepsilon_r > \varepsilon_\omega$, this condition is unacceptable; therefore, $\varepsilon_r = \omega_e/\omega_{nom}$ is adopted. In this case, the ICE torque does not depend on the position of the fuel supply control element.

Considering the above, the determination of the variation of the actual (effective) torque on the crankshaft is reduced to the calculation using the following formula:

$$M_e = M_{normz} \cdot M_{nom} + \frac{\varepsilon_r - \frac{\omega_e}{\omega_{nom}}}{k_x - 1} \cdot M_{nom} \qquad (4)$$

Taking this equation into account, we transform the general equation

$$J_e \cdot \frac{d\omega_e}{dt} = \left(M_{normz} + \frac{\varepsilon_r - \frac{\omega_e}{\omega_{nom}}}{k_x - 1}\right) \cdot M_{nom} + M_D \qquad (5)$$

It should be noted that the variation of the angular speed ω_e lies within the range $[\omega_{min}; k_x \cdot \omega_{nom}]$, while the variation of the fuel-supply control parameter ε_r lies within the range $[(\omega_{min} - M_{normz} \cdot \omega_{min} \cdot (k_x - 1))/\omega_{nom}; 1]$.

Thus, a mathematical description of the crankshaft's equation of motion in an internal combustion engine is presented, based on the dynamic equilibrium of a rotational system and generalizing Newton's second law to rotational motion.

To construct the fuel economy characteristics of the FPT NEF 67 internal combustion engine, the manufacturer's reference data are used, specifically the external speed characteristic consisting of the dependencies $M_e(\omega_1)$ and $N_e(\omega_1)$. The results are presented in Fig. 1.

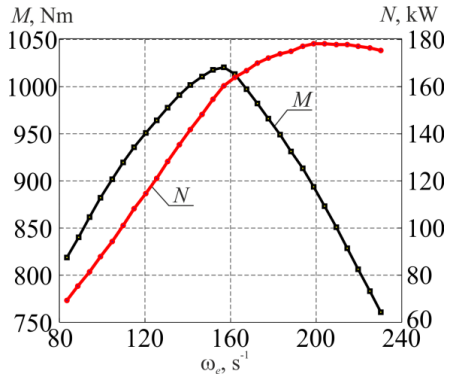

Fig. 1. External speed characteristic of the FPT NEF 67

The fuel consumption characteristics of any internal combustion engine depend on variations in the specific fuel consumption g_e, which is calculated using the equation:

$$g_e = g_{nom} \cdot k_\omega \cdot k_N \qquad (6)$$

where: g_{nom} – the nominal fuel consumption when the ICE operates in the nominal mode; k_ω – the coefficient characterizing the engine load with respect to the angular speed of the crankshaft; k_N – the coefficient characterizing the engine load with respect to power.

The following quadratic functions describe the dependencies of the engine load coefficients kω and kN

$$k_\omega = a_\omega + b_\omega \cdot \frac{\omega_e}{\omega_{nom}} + c_\omega \cdot \left(\frac{\omega_e}{\omega_{nom}}\right)^2 \qquad (7)$$

$$k_N = a_N + b_N \cdot \frac{N_e}{N_{e_{ESC}}} + c_N \cdot \left(\frac{N_e}{N_{e_{ESC}}}\right)^2 \qquad (8)$$

where: a_ω, b_ω, c_ω, a_N, b_N, c_N – constant coefficients; N_{e_ESC} – the effective engine power on the external speed characteristic at the same operating speed regime as N_e.

It should be noted that equations are valid under the following condition:

$$\begin{cases} a_\omega + b_\omega + c_\omega = 1; \\ a_N + b_N + c_N = 1. \end{cases} \quad (9)$$

After determining the specific fuel consumption, the instantaneous fuel consumption can be calculated.

$$G_M = 0.278 \cdot 10^{-6} \cdot g_e \cdot N_e \quad (10)$$

If it is necessary to determine the instantaneous fuel consumption over a certain time interval (from t_1 to t_2), the equation is transformed as follows:

$$G_M = 0.278 \cdot 10^{-6} \cdot \int_{t_1}^{t_2} g_e \cdot N_e dt \quad (11)$$

In addition to determining fuel consumption through the specific fuel consumption, it is also possible to calculate the effective efficiency of the internal combustion engine η_e, which is determined by the following equation,

$$\eta_e = \frac{3.6 \cdot 10^6}{g_e \cdot H_u} \quad (12)$$

where H_u is the lower heating value of the fuel.

Three-dimensional plots of the dependence of the effective power N_e and the specific fuel consumption g_e of the FPT NEF 67 internal combustion engine on the effective torque and the crankshaft angular speed are constructed. The results are shown in Fig. 2.

Analyzing the results shown in Fig. 2, it is noted that the maximum effective efficiency of the FPT NEF 67 ICE is 0.48, achieved at an effective torque Me = 750 Nm and a crankshaft angular speed ω_e = 178 s^{-1} (approximately 1700 rpm). Under these conditions, the specific fuel consumption g_e is 176 g/kWh, and the effective power N_e equals 124.75 kW.

The next step in determining the fuel characteristics of the internal combustion engine is to evaluate them using load characteristics.

4. Driving test cycles for wheeled tractors

One of the most important reasons for applying driving cycles is the impossibility of conducting a full-factorial experiment that would cover all possible combinations of rotational speed, load, temperature conditions, injection parameters, boosting modes, and control algorithms of the electronic control system. A full-factorial plan for an engine of such complexity as the NEF 67 would require thousands, or even tens of thousands, of experimental points, which is practically infeasible due to the enormous time and fuel consumption, engine wear, and the high requirements for measurement equipment. In addition, an experimental setup is not always capable of accurately reproducing the conditions under which a wheeled tractor, construction machine, or vehicle actually operates, especially with respect to abrupt load changes, road conditions, micro-transient processes, and the response of the boosting system.

Therefore, instead of full-factorial experiments, which are extremely complex, time-consuming, and practically unattainable for engines with wide load and rotational speed ranges, it is advisable to use standardized driving test cycles. For modeling the transport operation of wheeled tractors and other self-propelled machinery, the ELR (European Load Response [5]), EPA Nonregulatory Non-road Duty Cycles (Environmental Protection Agency [3]), and NRTC (Non-Road Transient Cycle [4]) cycles are widely applied. Each of these cycles is designed to reproduce different aspects of real engine operation, including variable loads, vehicle dynamics, and characteristic transient processes.

Since no single standardized transport cycle is specified for wheeled tractors, and their operation is often associated with movement in suburban conditions, the ELR cycle is appropriate for modeling the corresponding load modes. This cycle defines the response of the internal combustion engine to stepwise changes in crankshaft rotational speed and load (Fig. 3). This allows assessment of the dynamic characteristics of fuel supply during the transportation of trailed implements.

The essence of the ELR cycle is reduced to modeling the motion of a wheeled tractor at three speed operating modes (A, B, C) [5], which are defined as follows:

$$A = \omega_{minLO} + 0.25 \cdot (\omega_{maxHI} - \omega_{minLO}) \quad (13)$$

$$B = \omega_{minLO} + 0.5 \cdot (\omega_{maxHI} - \omega_{minLO}) \quad (14)$$

$$C = \omega_{minLO} + 0.75 \cdot (\omega_{maxHI} - \omega_{minLO}) \quad (15)$$

where ω_{minLO} is the minimum crankshaft angular speed of the internal combustion engine at 50% of the maximum engine power; ω_{maxHI} is the maximum crankshaft angular speed of the internal combustion engine at 70% of the maximum engine power.

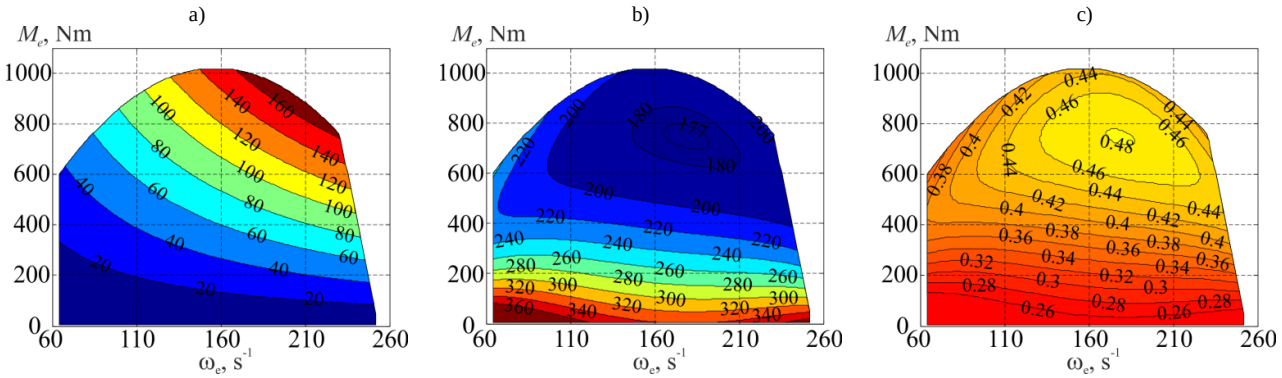

Fig. 2. Variation of the operating parameters of the FPT NEF 67 as functions of the effective torque M_e and the crankshaft angular speed ω_e: a) effective power N_e (kW); b) specific fuel consumption g_e (g/kWh); c) effective efficiency η_e

The EPA cycle (Fig. 3) is used to simulate the transport operating modes of a wheeled tractor or another self-propelled machine that operates on public roads or moves between production sites. It includes characteristic speed and load profiles typical of motion with steady-state sections, repeated accelerations, partial-load operation, and short transient processes. This makes the EPA cycle particularly valuable for evaluating fuel economy when a wheeled tractor operates as a transport vehicle rather than as a traction or working unit. In contrast to steady-state characteristics, the NRTC (Fig. 3) includes a complete sequence of realistic dynamic effects that occur during vehicle acceleration, transition to idle, shifts to partial loads, or operation at short-term peak power levels.

It should be noted that each of the above cycles has its own speed and load profile. In this research, only the speed characteristics of the cycle profiles are used, as the speed profile provides sufficient information, allowing modeling of changes in acceleration, deceleration and constant-speed motion, as well as the overall dynamic character of the transport operation. It is precisely the speed profile of the cycles that determines the duration of motion phases, the required tractive forces, and the subsequent energy consumption.

At the same time, the load profiles of the cycles (engine torque of the ICE) are less appropriate for studying the transport process with a towed tank, as they are derived from typical working operations involving variable technological modes and the operation of mounted implements. Such profiles describe the specific loading characteristics of the internal combustion engine during intensive, power-demanding operations, which do not correspond to the conditions of transport cargo movement, where tractive demand is determined by motion resistances, the unit's mass, and road conditions. In the case of a wheeled tractor with a towed tank, these loads can be calculated using a mathematical model of resistances and mass–inertia parameters rather than imposed by an external load cycle.

5. Investigation of changes in instantaneous fuel consumption

Before analyzing any research indicators, it is necessary to develop a general simulation model of a wheeled tractor towing a tank. For this purpose, we will use the MATLAB dynamic modeling system with the Simulink subsystem. The overall layout of the developed MATLAB/Simulink model is shown in Fig. 4. The general mathematical model of a wheeled tractor towing a tank is described by a system of differential equations. The calculation of these equations is based on time-component integration, which requires the use of a numerical method. Since the mathematical model is implemented in MATLAB, several numerical methods are available, including Euler (ode1), Heun (ode2), Bogacki-Shampine (ode3), Runge-Kutta (ode4), Dormand-Prince (ode5), and Dormand-Prince (ode8). We will select the classical Runge-Kutta method (ode4), which offers high accuracy at a moderate computational cost. The transported MGT-16 tank will reach a maximum speed of up to 20 km/h. Figure 5 shows the distribution of operating points of the change in the ICE's effective power during the simulation of the ELR, EPA, and NRTC cycles.

Analyzing the results in Fig. 5, it can be noted that for the ELR cycle, the operating points are generally localized around stabilized load conditions, without dynamic fluctuations or transient processes. The tractor essentially moves without load variation. In the EPA cycle, the operating points are concentrated over a wider range, closer to realistic transport conditions with stepwise changes in effective torque. Due to the absence of sharp load peaks, the "engine – transmission – wheels" system operates more stably and delivers traction more uniformly. In the NRTC cycle, the ICE's operating points are distributed much more broadly, covering both low and high values of torque and angular velocity. A particularly large number of points fall into the zone of transient loads and peak powers, where the engine produces abrupt, uneven traction values. This directly enhances the dynamic behavior of the "engine–transmission–wheels" system and, consequently, limits its ability to adapt to rapid load changes quickly.

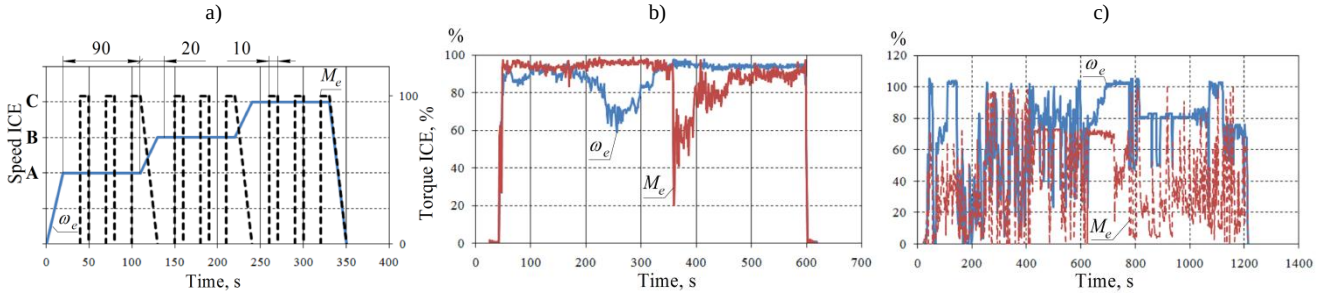

Fig. 3. Investigated driving test cycles of wheeled tractors: a) ELR; b) EPA; c) NRTC

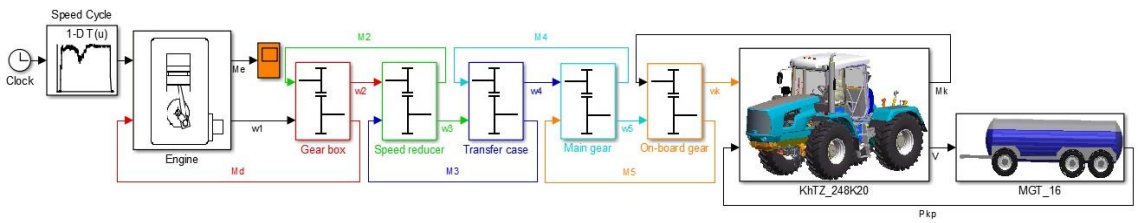

Fig. 4. Implementation of the KhTZ-248K.20 wheeled tractor and MGT-16 towed tank model in MATLAB/Simulink

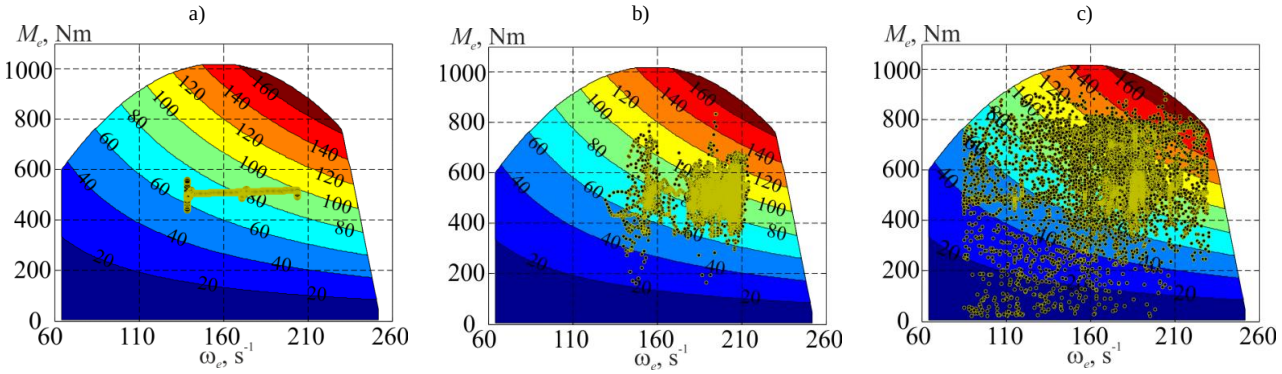

Fig. 5. Change in the distribution of operating points of the ICE's effective power during the simulation of driving cycles: a) ELR; b) EPA; c) NRTC

Considering the above, it becomes possible to determine the instantaneous fuel consumption of the ICE during the simulation of the ELR, EPA, and NRTC cycles. Analyzing the results from Fig. 6, it can be noted that during the simulation of the ELR cycle for the KhTZ-248K.20 wheeled tractor with a fully filled MGT-16 tank (H = 1.6 m or mp = 16 t), the instantaneous fuel consumption is G_M = 1631 g ≈ 1.6 kg. With an empty tank (H = 0 m or m_{liquid} = 0 kg), G_M = 568.5 g ≈ 0.6 kg.

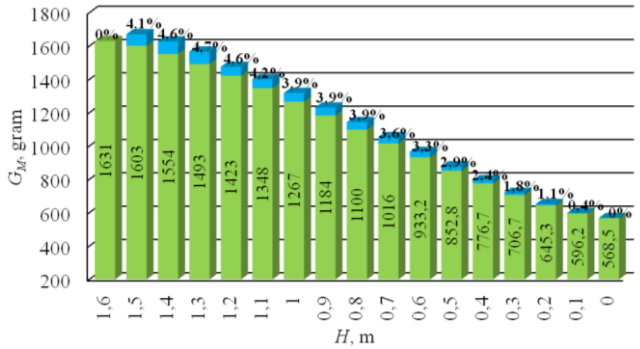

Fig. 6. Change in instantaneous fuel consumption GM during ELR cycle simulation depending on tank fill level H

Figure 6 shows the change in instantaneous fuel consumption when transporting the tank under the ELR cycle without considering the liquid's sloshing effects, as well as the percentage increase in fuel consumption when sloshing is accounted for. At extreme fill levels, no liquid motion occurs, whereas at intermediate levels, it affects the instantaneous fuel consumption. The greatest influence of liquid sloshing is observed when the tank is filled to H = 1.3 m, where G_M = 1567 g, which is 4.72% higher than the fuel consumption without considering sloshing. In Fig. 7, as in Fig. 6, the change in instantaneous fuel consumption is presented without considering liquid sloshing, and its increase when sloshing is included during the EPA cycle simulation. With a fully filled MGT-16 tank (H = 1.6 m), G_M = 3119 g. With an empty tank (H = 0 m), G_M = 1138 g. The greatest effect of liquid sloshing occurs at H = 1.3 m (the same trend as in the ELR cycle), where G_M = 3068 g, which is 6.76% higher than the fuel consumption without considering sloshing.

The increase in instantaneous fuel consumption at H = 1.3 m in the EPA cycle by 6.76%, compared to 4.72% in the ELR cycle, is due to the different dynamic structures of these test cycles. At H = 1.3 m, the liquid in the tank enters the most intensive longitudinal oscillation regime, as the fill level is close to resonance. This maximizes the amplitude of the liquid's center of mass motion, increasing inertial loads on the tractor during changes in engine speed and torque.

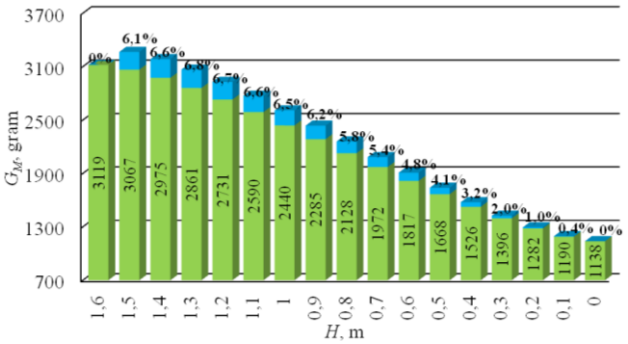

Fig. 7. Change in instantaneous fuel consumption G_M during EPA cycle simulation depending on tank fill level H

In the ELR cycle, the intensity of load and speed changes is moderate and smoother. Stepwise load increases without sharp accelerations or deep drops in instantaneous traction characterize this cycle. Therefore, the inertial forces generated by the liquid have a less pronounced effect on the engine, and the increase in fuel consumption is only 4.72%. In contrast, the EPA cycle contains a significantly larger number of rapid load changes, short-term peak regimes, and frequent transitions between acceleration, stabilization, and deceleration. Under these conditions, the sloshing mass of the liquid generates additional inertial moments that the tractor must compensate for, resulting in higher fuel consumption. Consequently, the fuel consumption increase reaches 6.76%.

In Fig. 8, as in Fig. 6 and Fig. 7, the change in instantaneous fuel consumption is shown without considering sloshing effects, and its increase when sloshing is taken into account during the NRTC cycle simulation. With a fully filled МЖТ-16 tank (H = 1.6 m), the instantaneous fuel consumption is G_M = 6508 g. With an empty tank (H = 0 m), G_M = 2600 g. The greatest influence of liquid sloshing occurs at a fill level of H = 1.3 m (the same trend observed in the ELR and EPA cycle simulations), where G_M = 6557 g, which is 9.22% higher than the fuel consumption without considering sloshing.

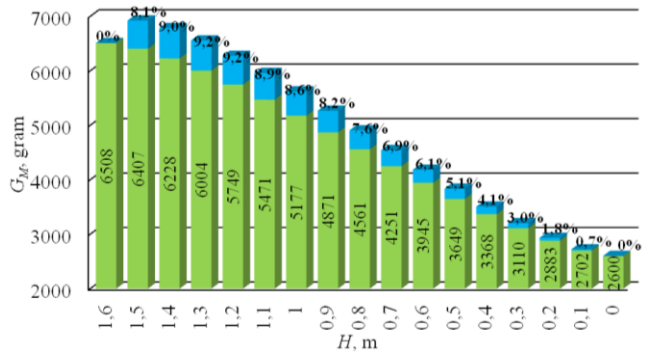

Fig. 8. Change in instantaneous fuel consumption G_M during NRTC cycle simulation depending on tank fill level H

The NRTC cycle exhibits high absolute fuel consumption, which is explained by its high energy intensity, high average power, and long duration. Consequently, the relative percentage increase is the largest because this cycle contains frequent, abrupt transient events whose spectrum closely matches the liquid's natural frequencies, leading to additional fuel consumption. In the EPA cycle, the relative percentage increase is smaller than in NRTC, because energy is expended to compensate for liquid accelerations, which constitute only a small portion of the already high baseline consumption, resulting in a 6.76% increase. The ELR cycle is the smoothest, so the liquid is minimally agitated, and both absolute and relative increases are the smallest.

The mechanism by which sloshing is converted into fuel consumption is that, during each acceleration or deceleration, the liquid must change its speed and position, performing inertial work that is powered by the ICE through increased fuel supply. The fill level H = 1.3 m is critical, as it corresponds to near-resonance conditions for the tank geometry, producing maximum liquid displacement amplitude and maximum additional inertial work.

The NRTC cycle yields the highest relative increase (9.22%), EPA the highest absolute but moderate relative increase (6.76%), and ELR the smallest (4.72%). Practically, this indicates that the fuel efficiency of transporting a filled tank depends not only on the fill level but also on the dynamics of motion, highlighting the importance of analyzing the transport of a partially filled tank with a tractor equipped with a hybrid transmission.

6. Conclusions

1. A mathematical representation of the fuel economy indicators of an internal combustion engine is presented, including instantaneous fuel consumption, volumetric fuel consumption, as well as the calculation of the effective efficiency factor, which is based on the determination of specific fuel consumption.

2. It is substantiated that determining the fuel characteristics of an internal combustion engine based on load characteristics makes it possible to evaluate its efficiency under real operating conditions, where rotational speed and torque continuously vary. This approach accounts for operating dynamics and transient processes, in contrast to fixed operating modes, and is practically necessary due to the complexity of conducting full-factorial experiments. Standardized driving cycles ELR, EPA, and NRTC make it possible to reproduce real operating conditions and assess fuel economy.

3. It is determined that the maximum increase in instantaneous fuel consumption GM during the transportation of the MGT-16 tanker is observed at a filling height of H = 1.3 m, which is caused by the inertial behavior of the liquid. For the ELR cycle, G_M (H = 1.3 m) = 1567 g, with a relative increase of 4.7% and an absolute increase of 74 g. For the EPA cycle, G_M (H = 1.3 m) = 3068 g, with a relative increase of 6.8% and an absolute increase of 207 g. For the NRTC cycle, G_M (H = 1.3 m) = 6557 g, with a relative increase of 9.2% and an absolute increase of 553 g. The largest relative increase occurs in the EPA cycle due to abrupt transient operating modes, the largest absolute increase occurs in the NRTC cycle due to its high energy intensity, and the smallest increase is observed in the ELR cycle due to smoother operating conditions.

Further research

In future work, experimental studies are planned under real road conditions, with traffic parameters recorded. This approach will allow verification of the adequacy of the mathematical model and simulation data, as well as the assessment of the impact of tank filling level on the tractor's fuel economy under variable traffic flow conditions. Additionally, the analysis is planned to be extended to different soil and road surface types, providing a more comprehensive understanding of the efficiency of transport operations in agricultural practice.

Acknowledgements

The study was carried out within the framework of the research project (No. 0125U000240) "Scientific underpinning of approaches to creating hybrid power plants for construction equipment".

Nomenclature

ICE	internal combustion engine	ELR	European Load Response
MTA	machine-tractor aggregate	EPA	Environmental Protection Agency
ESC	external speed characteristic	NRTC	non-road transient cycle

Bibliography

[1] Angelucci L, Mattetti M. The development of reference working cycles for agricultural tractors. Biosyst Eng. 2024; 242:29-37. https://doi.org/10.1016/j.biosystemseng.2024.04.004

[2] Antoshchenkov R, Halych I, Nykyforov A, Cherevatenko H, Chyzhykov I, Sushko S et al. Determining the influence of geometric parameters of the traction-transportation vehicle's

frame on its tractive capacity and energy indicators. East Eur J Enterp Technol. 2022;2(7):60-67. https://doi.org/10.15587/1729-4061.2022.254688
[3] United States Environmental Protection Agency. EPA non-regulatory non-road duty cycles. Washington (DC): EPA [cited 2026 Jan 9]. https://www.epa.gov/moves/epa-nonregulatory-nonroad-duty-cycles
[4] European Commission. Commission delegated regulation supplementing Regulation (EU) 2016/1628 with regard to technical and general requirements relating to emission limits and type-approval for internal combustion engines for non-road mobile machinery. Brussels 2016 [cited 2026 Jan 9]. https://eur-lex.europa.eu/legal-content/EN/TXT/?uri=PI_COM:Ares(2016)6327594
[5] European Load Response (ELR). DieselNet [cited 2026 Jan 9]. https://dieselnet.com/standards/cycles/elr.php
[6] Götz K, Kusuma A, Dörfler A, Lienkamp M. Agricultural load cycles: Tractor mission profiles from recorded GNSS and CAN bus data. Data Brief. 2025;60:111494. https://doi.org/10.1016/j.dib.2025.111494
[7] Jo S, Kim HJ, Kwon SI, Lee JT, Park S. Assessment of energy consumption characteristics of ultra-heavy-duty vehicles under real driving conditions. Energies. 2023;16: 2333. https://doi.org/10.3390/en16052333
[8] Kolodnenko V, Shyman A, Kalinin Y, Kuchuk N. Synthesis of the theory of motion of solid bodies filled with bulk substances for fault-tolerant identification of their parameters. 13th Int Conf Dependable Systems, Services and Technologies (DESSERT); 2023 October13-15; Athens. IEEE; 2023: 1-6. https://doi.org/10.1109/DESSERT61349.2023.10416449
[9] Kozhushko A. Hydrodynamics analysis on partially filled agricultural tanks by driving cycle of transportation. Ciboată DD (ed). International Conference on Reliable Systems Engineering (ICoRSE). Lecture Notes in Networks and Systems. 2023;762:259-270. Cham, Springer. https://doi.org/10.1007/978-3-031-40628-7_21
[10] Kozhushko A, Pelypenko Y, Kravchenko S, Danylenko V. Improving the procedure for modeling low frequency oscillations of the free surface liquid in a tractor tank. East Eur J Enterp Technol. 2023;122(7):61-68. https://doi.org/10.15587/1729-4061.2023.277254
[11] Kubín K, Pexa M, Holúbek M. Calculation model of the tractor transport set – economic and environmental indicators. Res Agric Eng. 2021;67(2):65-73. https://doi.org/10.17221/51/2020-RAE
[12] Lebedev A, Shuliak M, Khalin S, Lebedev S, Szwedziak K, Lejman K et al. Methodology for assessing tractor traction properties with instability of coupling weight. Agriculture. 2023;13:977. https://doi.org/10.3390/agriculture13050977
[13] Merkisz J. On-road exhaust emission testing. Combustion Engines. 2011;146(3):3-15. https://doi.org/10.19206/CE-117086
[14] Rahman SMA, Fattah IMR, Ong HC, Ashik FR, Hassan MM, Murshed MT et al. State-of-the-art of establishing test procedures for real driving gaseous emissions from light- and heavy-duty vehicles. Energies. 2021;14:4195. https://doi.org/10.3390/en14144195
[15] Reza S, Hassan S. Numerical simulation of half-full cylindrical and bi-lobed storage tanks against the sloshing phenomenon. Ocean Eng. 2022;266:112896. https://doi.org/10.1016/j.oceaneng.2022.112896
[16] Scolaro E, Beligoj M, Estevez MP, Alberti L, Renzi M, Mattetti M. Electrification of agricultural machinery: a review. IEEE Access. 2021;9:164520-41. https://doi.org/10.1109/ACCESS.2021.3135037
[17] United States Department of Agriculture. Agricultural Marketing Service. USDA agri-food supply chain assessment. Washington 2022 [cited 2026 Jan 9]. https://www.ams.usda.gov/sites/default/files/media/USDAAgriFoodSupplyChainReport.pdf
[18] Vezirov CZ, Atanasov AZ, Nikolova PD, Hristov KH. Informational support for agricultural machinery management in field crop cultivation. Agriculture. 2025;15:1356. https://doi.org/10.3390/agriculture15131356
[19] Wang W, Feng J, Wan W, Zhang P, Yang S. Modeling and analysis of the kinetic influence of liquid sloshing characteristics on high-clearance sprayers. Discrete Dyn Nat Soc. 2021;9926962:15. https://doi.org/10.1155/2021/9926962
[20] Yang H, Wu F, Gu F, Xu H, Shi L, Zhou X et al. Electric tractors in China: current situation, trends, and potential. World Electr Veh J. 2025;16:486. https://doi.org/10.3390/wevj16090486

Prof. Andrii Kozhushko, DSc., DEng. – Department of Car and Tractor Industry, National Technical University "Kharkiv Polytechnic Institute", Ukraine.
e-mail: *andrii.kozhushko@khpi.edu.ua*

Prof. Mykhailo Shuliak, DSc., DEng. – Department of Agroengineering, Sumy National Agrarian University. Ukraine.
e-mail: *m.l.shulyak@gmail.com*

Serhii Kravchenko, DEng. – Department of Engines and Hybrid Power Plants, National Technical University "Kharkiv Polytechnic Institute", Ukraine.
e-mail: *serhii.kravchenko@khpi.edu.ua*

Ivan Kolesnik, DEng. – Department of Tractors and Automobiles, National University of Life and Enviromental Sciences of Ukraine, Ukraine.
e-mail: *ivankolesnik@nubip.edu.ua*

Vitalii Danylenko – Department of Car and Tractor Industry, National Technical University "Kharkiv Polytechnic Institute", Ukraine.
e-mail: *vitalii.ddanylenko@gmail.com*